Glutamine deprivation triggers NAGK-dependent hexosamine salvage

Campbell, S.L.[1,2], Mesaros, C.[3], Affronti, H.[1,2], Tsang, T.[1,2], Noji, M.[1,2], Sun, K.[4], Izzo, L.[1,2], Trefely, S.[1,2,5], Kruijning, S.[1,2], Blair, I.A.[3], Wellen, K.E.[1,2,6]

[1]Department of Cancer Biology, [2]Abramson Family Cancer Research Institute, [3]Department of Systems Pharmacology and Translational Therapeutics, [4]Pancreatic Cancer Research Center, Perelman School of Medicine, University of Pennsylvania; [5]Center for Metabolic Disease Research, Department of Microbiology and Immunology, Lewis Katz School of Medicine, Temple University, Philadelphia, PA 19140. [6]Corresponding author.

Abstract

Tumors of many types exhibit aberrant glycosylation, which can impact cancer progression and therapeutic responses. The hexosamine biosynthesis pathway (HBP) branches from glycolysis at fructose-6-phosphate to synthesize uridine diphosphate N-acetylglucosamine (UDP-GlcNAc), a major substrate for glycosylation in the cell. HBP enzyme gene expression is elevated in pancreatic ductal adenocarcinoma (PDA), and studies have pointed to the potential significance of the HBP as a therapeutic target. Yet, the PDA tumor microenvironment is nutrient poor, and adaptive nutrient acquisition strategies support tumorigenesis. Here, we identify that pancreatic cancer cells salvage GlcNAc via N-acetylglucosamine kinase (NAGK), particularly under glutamine limitation. Glutamine deprivation suppresses *de novo* HBP flux and triggers upregulation of *NAGK*. *NAGK* expression is elevated in human PDA. *NAGK* deletion forces PDA cells to rely on *de novo* UDP-GlcNAc synthesis and impairs tumor growth in mice. Together, these

This manuscript has been co-submitted with Kim et al. (2020), "Pancreatic Cancers Scavenge Hyaluronic Acid to Support Growth."

data identify an important role for NAGK-dependent hexosamine salvage in supporting PDA tumor growth.

INTRODUCTION

Altered glycosylation is frequently observed in malignancies, impacting tumor growth as well as immune and therapeutic responses (Akella et al., 2019; Mereiter et al., 2019). Several types of glycosylation, including O-GlcNAcylation and N-linked glycosylation, are dependent on the glycosyl donor uridine diphosphate N-acetylglucosamine (UDP-GlcNAc), which is synthesized by the hexosamine biosynthesis pathway (HBP). The HBP branches off from glycolysis with the transfer of glutamine's amido group to fructose-6-phosphate (F-6-P) to generate glucosamine-6-phosphate (GlcN-6-P), mediated by the rate limiting enzyme glutamine—fructose-6-phosphate transaminase (GFPT1/2). The pathway further requires acetyl-CoA, ATP, and uridine triphosphate (UTP) to ultimately generate UDP-GlcNAc. O-GlcNAcylation, the addition of a single N-acetylglucosamine (GlcNAc) moiety onto a serine or threonine residue of intracellular proteins, is upregulated in multiple cancers (Akella, et al., 2019). Targeting O-GlcNAcylation suppresses the growth of breast, prostate, and colon cancer tumors (Caldwell et al., 2010; Ferrer et al., 2017; Gu et al., 2010; Guo et al., 2017; Lynch et al., 2012). Similarly, certain N-glycan structures (e.g., tetra-antennary N-glycans) are highly sensitive to HBP flux and are upregulated in malignant tissue, and targeting the relevant glycan remodeling enzymes can limit tumor growth and metastasis in vivo (Granovsky et al., 2000; Li et al., 2008; Zhou et al., 2011). Thus, understanding the regulation of the HBP in cancer could point towards novel therapeutic strategies.

Pancreatic ductal adenocarcinoma (PDA) is a deadly disease with a 5-year survival rate of 9% and a rising number of annual deaths (Rahib et al., 2014) (ACS Cancer Facts and Figures 2019, NIH SEER report 2019). Mutations in *KRAS* occur in nearly all cases of human PDA and drive extensive metabolic reprogramming in cancer cells. Enhanced flux into the HBP was identified as

a primary metabolic feature mediated by mutant KRAS in PDA cells (Ying et al., 2012). Hypoxia, a salient characteristic of the tumor microenvironment (Lyssiotis & Kimmelman, 2017), was shown to further promote expression of glycolysis and HBP genes in pancreatic cancer cells (Guillaumond et al., 2013). Notably, the glutamine analog 6-diazo-5-oxo-L-norleucine (DON), which inhibits the HBP, suppressed PDA metastasis and sensitized PDA tumors to anti-PD-L1 therapy (Sharma et al., 2020). DON has also been reported to sensitize PDA cells to the chemotherapeutic gemcitabine in vitro (Chen et al., 2017). Additionally, a recently developed inhibitor targeting the HBP enzyme phosphoacetylglucosamine mutase 3 (PGM3) enhances gemcitabine-mediated reduction of xenograft tumor growth in vivo (Ricciardiello et al., 2020). Thus, the HBP may represent a therapeutic target in PDA, although the regulation of UDP-GlcNAc synthesis and the optimal strategies to target this pathway for therapeutic benefit in PDA remain poorly understood.

An outstanding question is the impact of the tumor microenvironment on UDP-GlcNAc synthesis. The HBP has been proposed as a nutrient-sensing pathway since its rate-limiting step, mediated by GFPT1/2, requires both glutamine and the glycolytic intermediate fructose-6-phosphate (Denzel & Antebi, 2015). In hematopoietic cells, glucose deprivation limits UDP-GlcNAc levels and dramatically reduces levels of the N-glycoprotein IL3Rα at the plasma membrane in a manner dependent on the HBP (Wellen et al., 2010). Similarly, O-GlcNAcylation of certain nuclear-cytosolic proteins, including cancer-relevant proteins such as Myc and Snail, has been demonstrated to be nutrient sensitive, impacting protein stability or function (Housley et al., 2008; Park et al., 2010; Swamy et al., 2016). Yet, the PDA tumor microenvironment is thought to be particularly nutrient poor, owing to its characteristic dense stroma (Halbrook & Lyssiotis, 2017). This raises the question of how nutrient deprivation impacts the synthesis of UDP-GlcNAc and its utilization for glycosylation. Understanding how PDA cells regulate these processes under nutrient limitation could identify therapeutic vulnerabilities. In this study, we investigated the impact of

nutrient deprivation on the HBP and glycosylation in PDA cells, identifying a key role for hexosamine salvage through the enzyme N-acetylglucosamine kinase (NAGK) in PDA tumor growth.

MATERIALS AND METHODS

Cell culture

Cells were cultured in DMEM high glucose (Gibco, 11965084) with 10% calf serum (Gemini GemCell U.S. Origin Super Calf Serum, 100-510), unless otherwise noted. Glucose- or glutamine-restricted media was prepared using glucose, glutamine, and phenol red free DMEM (Gibco, A1443001) supplemented with glucose (Sigma-Aldrich, G8769), glutamine (Gibco, 25030081), and dialyzed fetal bovine serum (Gemini, 100-108). 1% oxygen levels were achieved by culturing cells in a Whitley H35 Hypoxystation (Don Whitley Scientific). ATCC names and numbers for the cell lines used in this study are: MIA PaCa-2 (ATCC# CRL-1420), Panc-1 (ATCC# CRL-1469), HPAC (ATCC# CRL-2119), AsPC-1 (ATCC# CRL-1682), BxPC-3 (ATCC# CRL-1687), HCT 116 (ATCC# CCL-247), and SW480 (ATCC# CCL-228). All cells were routinely tested for mycoplasma and authenticated by short tandem repeat (STR) profiling using the GenePrint 10 System (Promega, B9510).

Generation of CRISPR cell lines

sgRNA sequences targeting *NAGK* or *Mgat5* from the Brunello and Brie libraries (Doench et al., 2016) were cloned into the lentiCRISPRv2 vector (Sanjana, Shalem et al., 2014). Lentivirus was produced in 293T cells according to standard protocol. Cells were then infected with the CRISPR lentivirus and selected with puromycin. Cells were plated at very low density into 96 well plates to establish colonies generated from single cell clones. *Mgat5* gene disruption was validated by qPCR and L-PHA binding. *NAGK* gene disruption was validated by qPCR and western blot. Four

NAGK knockout clonal cell lines established from two different sgRNAs were chosen for use in the study. Please see table at end of methods for primer sequences of guides used.

Western blotting

For protein extraction from cells, cells were kept on ice and washed three times with PBS, then scraped into PBS and spun down at 200g for 5 minutes. The cell pellet was resuspended in 50-100 μL RIPA buffer [1% NP-40, 0.5% deoxycholate, 0.1% SDS, 150 mM NaCl, 50 mM Tris plus protease inhibitor cocktail (Sigma-Aldrich, P8340) and phosSTOP (Sigma-Aldrich, 04906845001)] and lysis was allowed to continue on ice for 10 minutes. Cells were sonicated with a Fisherbrand Model 120 Sonic Dismembrator (Fisher Scientific, FB120A110) for three pulses of 20 seconds each at 20% amplitude. Cell lysate was spun down at 15,000g for 10 minutes at 4°C and supernatant was transferred to a new tube. For protein extraction from tissue, the sample was resuspended in 500 μL RIPA buffer and homogenized using a TissueLyser (Qiagen, 85210) twice for 30s at 20 Hz. Following incubation on ice for 10 minutes the same procedure was followed as for cells. For both cells and tissue, lysate samples were stored at -80°C until analysis by immunoblot. All blots were developed using a LI-COR Odyssey CLx system. Antibodies used in this study were: O-GlcNAc CTD110.6 (Cell Signaling 9875S), tubulin (Sigma T6199), HSP60 (Cell Signaling 12165S), and NAGK (Atlas Antibodies, HPA035207).

RT-qPCR

For RNA extraction from cells, cells were put on ice, washed with PBS, and scraped into PBS. Samples were then spun down at 200g for 5 minutes and resuspended in 100 μL Trizol (Life Technologies). For RNA extraction from tissue, samples were resuspended in 500 μL Trizol and homogenized using a TissueLyser twice for 30s at 20 Hz. For both cells and tissue, RNA was extracted following the Trizol manufacturer protocol. cDNA was prepared using high-capacity RNA-to-cDNA master mix (Applied Biosystems, 4368814) according to kit instructions. cDNA was

diluted 1:20 and amplified with PowerUp SYBR Green Master Mix (Applied Biosystems, A25778) using a ViiA-7 Real-Time PCR system. Fold change in expression was calculated by the $\Delta\Delta C_t$ method using HPRT as a control. Please see table at end of methods for primer sequences.

Lectin binding assay

Cells were put on ice, washed with PBS and then scraped into PBS. Samples were then spun down at 200g for 5 minutes and resuspended in 3% BSA with fluorophore-conjugated lectin added 1:1000. Samples were covered and incubated on ice for 30 minutes at room temperature, then spun down and resuspended in PBS before analysis with an Attune NxT Flow Cytometer (Thermo Fisher Scientific). Data was further analyzed using FlowJo 8.7.

Metabolite quantitation and labeling

Samples were prepared according to Guo et al. (Guo et al., 2016). Briefly, cells were put on ice and washed 3x with PBS. Then, 1 mL of ice cold 80% methanol was added to the plate, and cells were scraped into solvent and transferred to a 1.5 mL tube. For quantitation experiments, internal standard containing a mix of ^{13}C labeled metabolites was added at this time. Samples were then sonicated and spun down, and the supernatants were dried down under nitrogen. The dried samples were then resuspended in 100 μL of 5% sulfosalicylic acid and analyzed by liquid chromatography-high resolution mass spectrometry as reported (Guo et al., 2016) with the only modification that the LC was coupled to a Q Exactive-HF with a heated ESI source operating in negative ion mode alternating full scan and MS/MS modes. The $[M-H]^-$ ion of each analyte and its internal standard was quantified, with peak confirmation by MS/MS. Data analysis was conducted in Thermo XCalibur 3.0 Quan Browser and FluxFix (Trefely et al., 2016).

For glucose labeling experiments, cells were cultured in DMEM without glucose, glutamine, or phenol red supplemented with 10 mM [U-^{13}C]-glucose (Cambridge Isotopes, CLM-1396-1), 4 mM glutamine, and 10% dialyzed fetal bovine serum. Cells were incubated for the indicated time, and

samples were prepared as above. For GlcNAc labeling experiments, cells were cultured in DMEM without glucose, glutamine, or phenol red supplemented with 10 mM N-[1,2-13C2]acetyl-D-glucosamine (^{13}C GlcNAc) (Omicron Biochemicals, GLC-006), 4 mM glutamine, 10 mM glucose, and 10% dialyzed fetal bovine serum. Cells were incubated for the indicated time, and samples were prepared as above.

Soft agar colony formation assay

Cells were trypsinized and counted using a Bright-Line hemacytometer (Sigma, Z359629). The bottom agar layer was prepared by adding Bacto Agar (BD Bioscience, 214050) to cell culture media for a final concentration of 0.6%. 2 mL bottom agar was added to each well of a 6-well tissue culture plate. Once bottom agar solidified, top layer agar was prepared by combining trypsinized cells with the bottom agar mix for a final concentration of 0.3% Bacto Agar. 1 mL top layer agar was added to each well with a bottom layer of agar. Cells were plated $2.5x10^4$ per well. 0.5 mL DMEM high glucose with 10% calf serum was added to cells every 7 days. Images were taken after 3 weeks. Images were blinded and colonies per image were counted using ImageJ (Schneider, Rasband, & Eliceiri, 2012).

2D Proliferation assay

Cells were plated $3.5x10^4$ per well of a 6-well plate. For each day that counts were recorded, three wells were trypsinized and cells were counted twice using a hemocytometer (Sigma, Z359629). The average of the two counts was recorded for each well, and the average count of the three wells was used to graph the data.

Bioinformatics data analysis

The PDAC expression profiling dataset (GEO accession GSE16515, Pei et al., 2009) from NCBI GEO Profile database (Edgar et al., 2002) was used to compare the expression level between

human normal and PDAC tumor samples. The dataset consists of 52 samples, in which 16 samples are matched tumor and normal tissues, and 20 samples are only tumor tissues. The statistical analysis was conducted by one-way ANOVA, the level of significance was evaluated by $p < 0.01$ and plotted in box-and-whisker diagram. Comparison of HBP gene expression between tumor (TCGA PAAD dataset) and normal tissue (GTEx) was also conducted using GEPIA2 (Tang et al., 2019).

Tumor growth in vivo

$3x10^6$ PANC-1 NAGK CRISPR cells were injected with 1:1 Matrigel (Corning, CB354248) into the flanks of NCr nude mice and measured with calipers once per week for 22 weeks. At the experiment endpoint (22 weeks or when tumor reached 20 mm in length), mice were euthanized with CO_2 and cervical dislocation. Tumors were removed, weighed, cut into pieces for analysis, and frozen. All animal experiments were approved by the University of Pennsylvania and the Institutional Animal Care and Use Committee (IACUC).

	Primers	
qPCR	*GFPT1* forward	CTCTGGCTTTGGTGGATAAA
	GFPT1 reverse	GCAACCACTTGCTGAAGA
	NAGK forward	GTGCTCATATCTGGAACAGG
	NAGK reverse	ACCCTCATCACCCATCATA
	HPRT forward	ATTATGCCGAGGATTTGGAA
	HPRT reverse	CCCATCTCCTTCATGACATCT
	RPL19 forward	CAAGAAGGAGGAGATCATCAAG
	RPL19 reverse	ATCACAGAGGCCAGTATGTA
CRISPR	sgMGAT5 mouse forward	CACCGGCTGTCATGACACCAGCGTA
	sgMGAT5 mouse reverse	AAACTACGCTGGTGTCATGACAGCC
	sgNAGK#1 forward	CACCGTTGACGTAGCCGATATCATG
	sgNAGK#1 reverse	AAACCATGATATCGGCTACGTCAAC
	sgNAGK#2 forward	CACCGTGCTTGGTGTGCGATCCAGT
	sgNAGK#2 reverse	AAACACTGGATCGCACACCAAGCAC

RESULTS

This manuscript has been co-submitted with Kim et al. (2020), "Pancreatic Cancers Scavenge Hyaluronic Acid to Support Growth."

Tetra-antennary N-glycans and O-GlcNAcylation are minimally impacted by nutrient limitation in pancreatic cancer cells

To examine the effects of nutrient deprivation on glycosylation in PDA cells, we cultured the cells in low glucose or low glutamine conditions and examined O-GlcNAc levels, as well as cell surface phytohemagglutinin-L (L-PHA) binding, a readout of N-acetylglucosaminyltransferase 5 (MGAT5)-mediated cell surface N-glycans (Fig S1A,B), which are highly sensitive to UDP-GlcNAc availability (Lau et al., 2007). We focused on glucose and glutamine because of their requirement to initiate the HBP (Fig. 1A). As a positive control, we examined HCT-116 and SW480 colon cancer cells, previously documented to have glucose-responsive O-GlcNAcylation (Park et al., 2010; Steenackers et al., 2016), which we also confirmed in HCT-116 cells (Fig. S1C). Indeed, LPHA binding was suppressed by glucose restriction in SW480 cells and by glutamine restriction in both colon cancer cell lines (Fig. 1B). To test whether glycans were sensitive to nutrient restriction in pancreatic cancer cells, we examined LPHA binding and O-GlcNAc levels under nutrient deprivation conditions in a panel of human PDA cell lines, including PANC-1, MIA PaCa-2, AsPC-1, and HPAC. Across these cell lines, no consistent changes in L-PHA binding were observed under glucose or glutamine limitation (Fig. 1C, D; Fig. S1D). We also examined L-PHA binding in PDA cells under oxygen- or serum-deprived conditions and observed again that levels were overall maintained (Figure 1E, F). O-GlcNAcylation was minimally altered by culture in low glutamine and exhibited variable changes in response to glucose limitation (Fig. 1G), consistent with stress-induced regulation of this modification (Taylor et al., 2008). Thus, under a variety of nutrient stress conditions, neither L-PHA binding nor O-GlcNAcylation were consistently suppressed in pancreatic cancer cell lines. Glutamine restriction in particular had remarkably little impact on O-GlcNAcylation and L-PHA binding, raising the question of how glycosyl donors are generated during nutrient limitation.

This manuscript has been co-submitted with Kim et al. (2020), "Pancreatic Cancers Scavenge Hyaluronic Acid to Support Growth."

Pancreatic cancer cells generate UDP-GlcNAc through salvage

Since UDP-GlcNAc is synthesized de novo through the HBP, we next asked whether abundance of HBP metabolites is impacted by nutrient limitation. We measured HBP metabolites after glucose or glutamine restriction using HPLC-MS (Guo et al., 2016). In low glutamine conditions,

This manuscript has been co-submitted with Kim et al. (2020), "Pancreatic Cancers Scavenge Hyaluronic Acid to Support Growth."

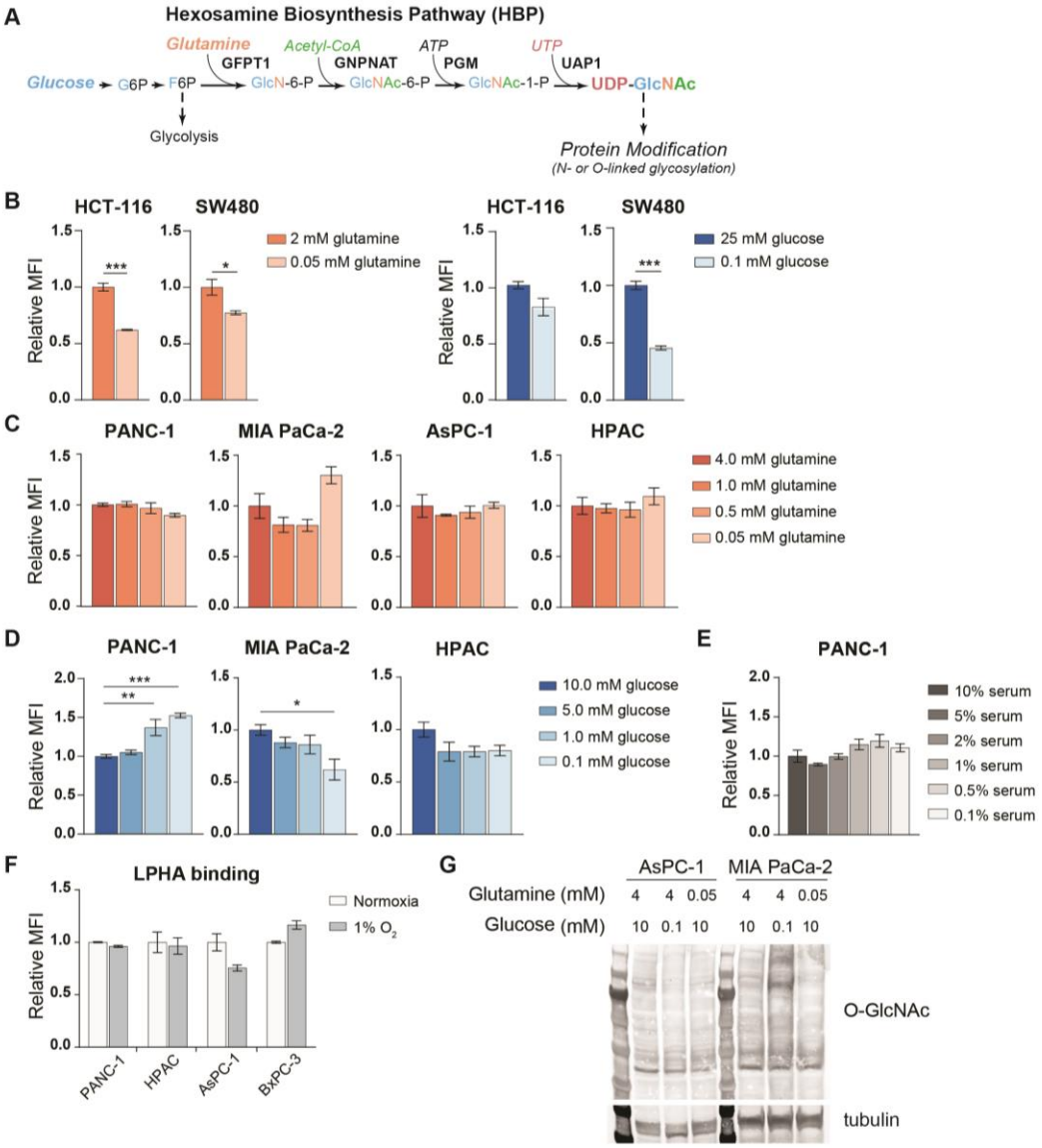

Figure 1: MGAT5-dependent N-glycans are minimally impacted by glucose or glutamine deprivation in PDA cells.

A) Overview of the hexosamine biosynthesis pathway (HBP). **B)** Phytohemagglutinin-L (LPHA) binding in colon cancer cells. Cells were incubated in the indicated concentrations of glutamine (left) or glucose (right) for 48 hours and then analyzed by flow cytometry. Statistical significance was calculated by unpaired t-test. **C-F)** Phytohemagglutinin-L (LPHA) binding in pancreatic ductal adenocarcinoma (PDA) cells in low nutrients. Cells were incubated in the indicated concentrations of glutamine (C), glucose (D), serum (E), or oxygen (F) for 48 hours and then analyzed by flow cytometry. Statistical significance was calculated by one-way ANOVA. **G)** O-GlcNAc levels in PDA cells in high and low nutrients. Cells were incubated in the indicated concentrations of glucose or glutamine for 48 hours. For all bar graphs, mean +/- standard error of the mean (SEM) of three biological triplicates is represented. Panels B) - G) are representative of at least two independent experimental replicates. *, $p \leq 0.05$; **, $p \leq 0.01$; ***, $p \leq 0.001$.

GlcN-6-P levels were potently decreased relative to 4 mM glutamine while UDP-GlcNAc abundance was maintained (Fig 2A), indicating that UDP-GlcNAc might be generated through mechanisms other than de novo synthesis under glutamine limitation. Glycolytic intermediates fructose-1,6-bisphosphate and pyruvate were minimally impacted by low glutamine conditions,

This manuscript has been co-submitted with Kim et al. (2020), "Pancreatic Cancers Scavenge Hyaluronic Acid to Support Growth."

and TCA cycle intermediates such as α-KG decreased as expected (Fig. S2A). In contrast to glutamine restriction, UDP-GlcNAc was not maintained under glucose limitation (Fig. S2B), suggesting that glutamine limitation specifically may trigger an adaptive response to sustain UDP-GlcNAc pools.

We sought to understand how UDP-GlcNAc pools are sustained during glutamine restriction. To investigate the possibility that UDP-GlcNAc is generated through mechanisms other than its synthesis from glucose, we designed an isotope labeling strategy to determine the fraction of the glucosamine ring that is synthesized *de novo*. Since multiple components of UDP-GlcNAc [glucosamine ring, acetyl group, uridine (both the uracil nucleobase and the ribose ring)] can be synthesized from glucose, UDP-GlcNAc isotopologues up to M+17 can be generated (Moseley et al., 2011) (Fig. 2B). In order to measure the glucose carbon incorporated into UDP-GlcNAc via the HBP, all isotopologues containing a fully labeled glucosamine ring, or M+6, are added together (Fig. 2B). After 48 hours of glutamine restriction, cells were incubated with fresh low glutamine medium containing [U-^{13}C]-glucose to track the incorporation of glucose carbons into hexosamine intermediates. The fractional labeling of both GlcNAc-P and UDP-GlcNAc pools was significantly suppressed by glutamine restriction, indicating decreased de novo synthesis in low glutamine conditions (Fig. 2C, Fig. S2C, D). Labeling of F-6-P in contrast was not impacted by glutamine restriction (Fig. 2C, Fig. S2E). Of note, M+6 UDP-GlcNAc could also be generated in principle through 6 carbons in UTP becoming labeled (e.g. 5 carbons in ribose and 1 carbon in uracil); however this is minimally observed in UTP labeling (Fig. S2F), indicating that the majority of M+6 UDP-GlcNAc reflects labeling in the glucosamine ring. Thus, UDP-GlcNAc abundance is maintained under glutamine restriction (Fig. 2A) despite reduced *de novo* synthesis from glucose (Fig. 2C).

This manuscript has been co-submitted with Kim et al. (2020), "Pancreatic Cancers Scavenge Hyaluronic Acid to Support Growth."

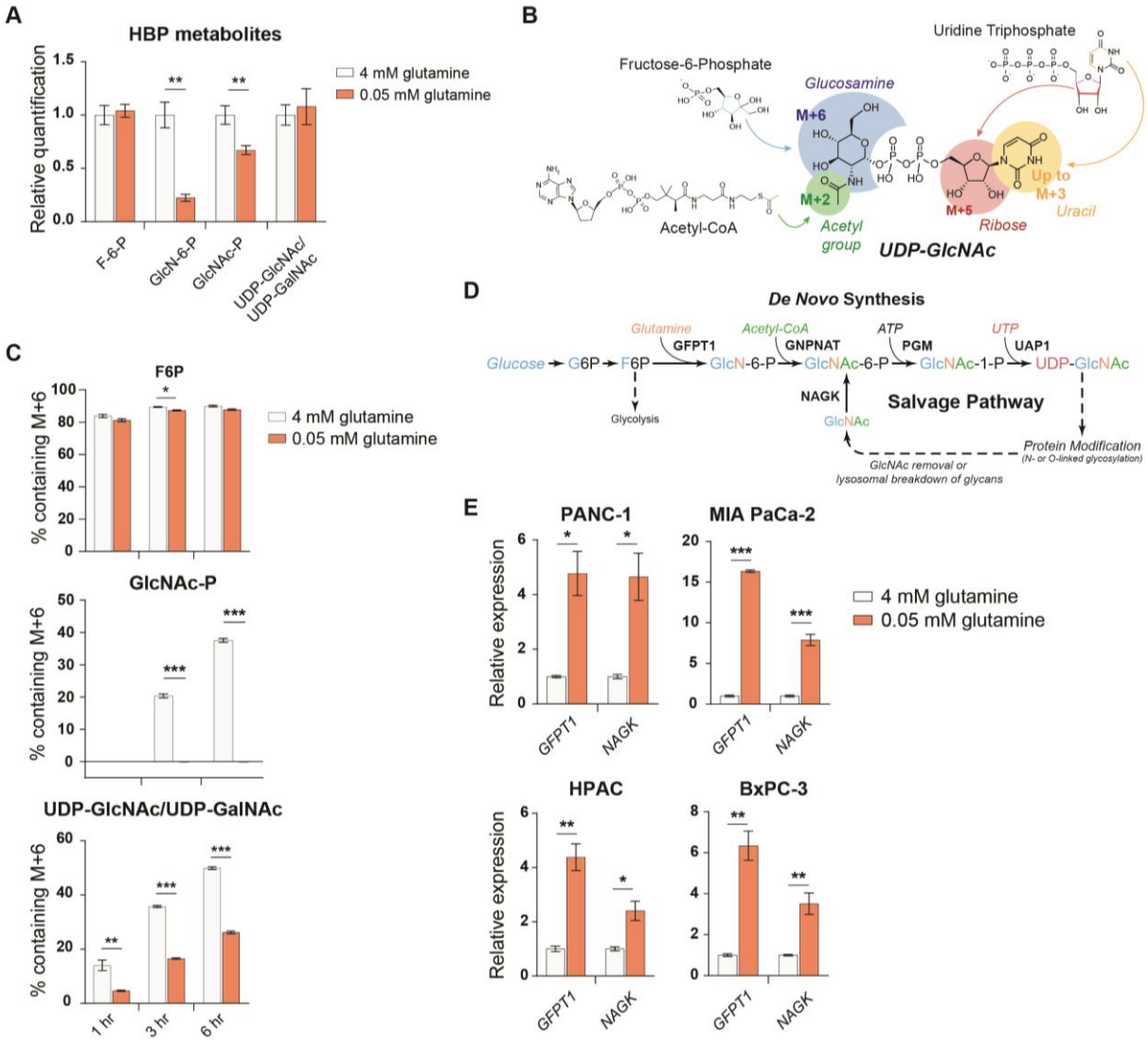

Figure 2: UDP-GlcNAc levels are maintained in low glutamine conditions despite reduced *de novo* hexosamine synthesis.

A) Measurement of HBP metabolites in PANC-1 cells. Cells were cultured in 0.05 mM glutamine for 48 hours, then metabolites were extracted and samples were analyzed by HPLC-MS. Statistical significance was calculated by unpaired t-test. Mean +/- SEM of five biological replicates is represented. B) Overview of the incorporation of ^{13}C glucose into UDP-GlcNAc. Different parts of the molecule can be labeled from glucose-derived subunits, thus isotopologues up to M+17 can be observed. C) Percent of F-6-P, GlcNAc-P, and UDP-GlcNAc isotopologues containing M+6 under the indicated concentrations of glutamine. In GlcNAc-P and UDP-GlcNAc, the M+6 isotopologue is generated from a labeled glucosamine ring, indicating *de novo* synthesis of UDP-GlcNAc. All isotopologues are graphed in Figure S2. Statistical significance was calculated by unpaired t-test. Mean +/- SEM of three biological replicates is represented. D) Overview of the GlcNAc salvage pathway feeding into the HBP. GlcNAc scavenged from O-GlcNAc removal or lysosomal breakdown of glycans can be phosphorylated by NAGK and used to regenerate UDP-GlcNAc. E) Gene expression of *GFPT1* and *NAGK* in PDA cells cultured in the indicated concentrations of glutamine. Statistical significance was calculated by unpaired t-test. Mean +/- SEM of three biological replicates is represented. All panels are representative of at least two experimental replicates. *, p≤ 0.05; **, p ≤ 0.01; ***, p ≤ 0.001.

UDP-GlcNAc can also be generated via phosphorylation of GlcNAc by N-acetylglucosamine kinase (NAGK), generating GlcNAc-6-P (Fig. 2D). Sources of GlcNAc in the cell may include

This manuscript has been co-submitted with Kim et al. (2020), "Pancreatic Cancers Scavenge Hyaluronic Acid to Support Growth."

removal of O-GlcNAc protein modifications or breakdown of glycoconjugates and extracellular matrix components. Yet, the significance of NAGK to maintenance of UDP-GlcNAc pools has been little studied, and the proportion of UDP-GlcNAc generated via the NAGK-dependent salvage pathway is unknown. Notably, *NAGK* expression increased in PDA cell lines in low glutamine conditions (Fig. 2E). *NAGK* was upregulated in some but not all cell lines with glucose restriction (Fig. S2G). *GFPT1* expression was induced in both low glucose conditions, consistent with a prior report (Moloughney et al., 2016), and in low glutamine conditions (Fig. 2E; Fig. S2G). These data indicate that under low glutamine conditions, *de novo* hexosamine synthesis from glucose is reduced, but expression of the salvage pathway enzyme *NAGK* increases.

NAGK deficiency reveals inherent flexibility between hexosamine synthesis and salvage

These findings prompted us to investigate the role of NAGK in UDP-GlcNAc synthesis in PDA cells. We functionally examined the role of NAGK in PDA cell lines by using CRISPR-Cas9 gene editing to generate NAGK knockout (KO) PANC-1 cell lines (Fig. S3A, B). By tracing 10 mM N-[1,2-$^{13}C_2$]acetyl-D-glucosamine (^{13}C GlcNAc) into the UDP-GlcNAc pool, we confirmed that NAGK deletion suppressed GlcNAc salvage, as evidenced by reduced fractional labeling of GlcNAc-P and UDP-GlcNAc from ^{13}C GlcNAc (Fig. 3A). As expected, no ^{13}C GlcNAc was incorporated into F-6-P (Fig. S3C). We hypothesized that knockout cells would conduct increased de novo UDP-GlcNAc synthesis. To test this, we incubated cells with [U-^{13}C]-glucose and examined incorporation into GlcNAc-P and UDP-GlcNAc. Indeed, we observed increased fractional labeling of hexosamine intermediates including UDP-GlcNAc and GlcNAc-P from glucose in the absence of NAGK (Fig. 3B-C; Fig. S3D-E). This effect was also observed with knockdown of NAGK by shRNA, though to a lesser extent (Fig. S3F-G). Importantly, incorporation of glucose into F-6-P did not change (Fig. 3C) and the proportion of UDP-GlcNAc containing an m+5 ribose ring was unchanged in knockout cells (Fig. 3B), indicating that NAGK specifically impacts glucose flux into

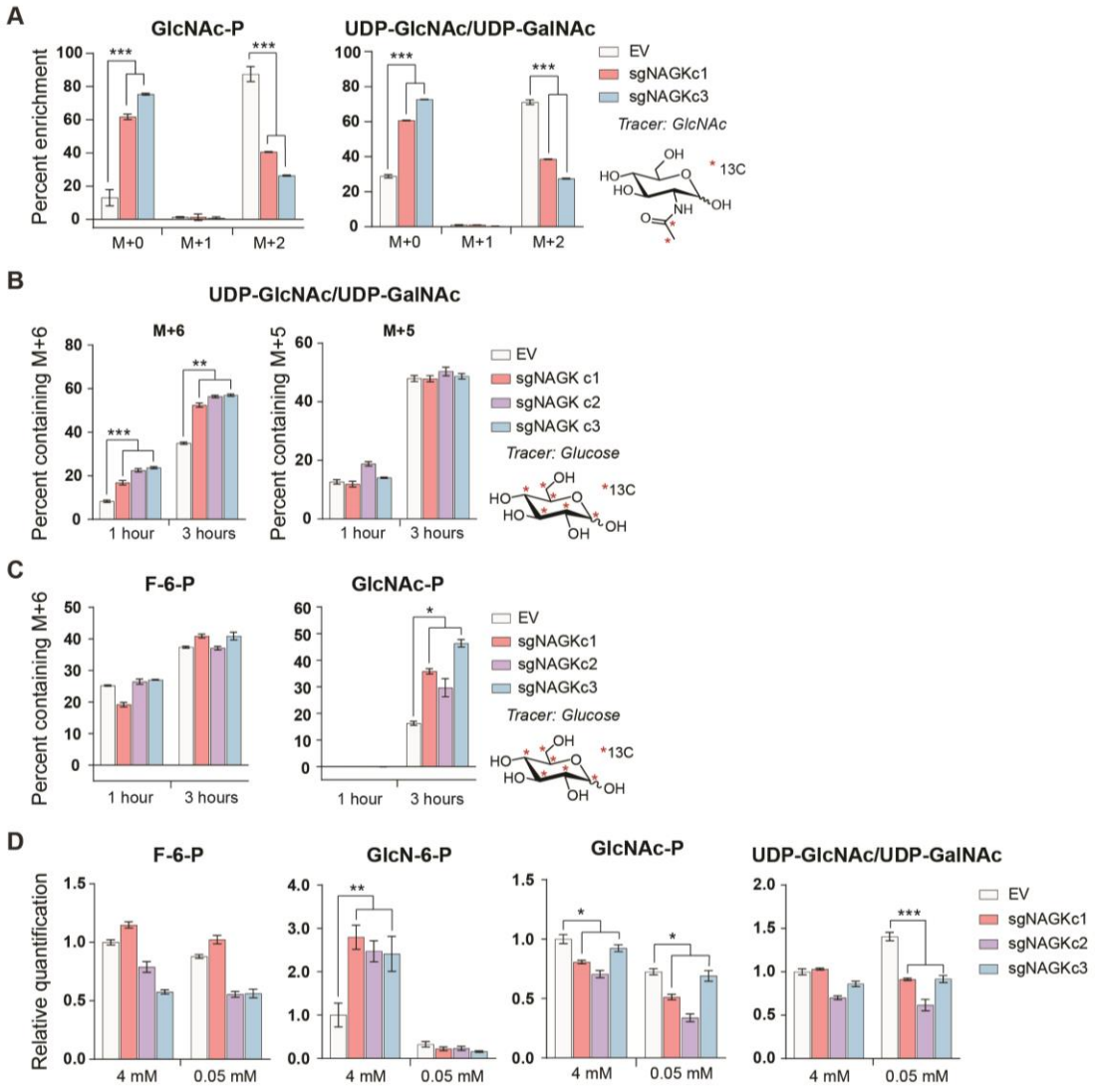

Figure 3: NAGK deletion increases *de novo* hexosamine synthesis.

A) Measurement of ^{13}C GlcNAc labeled on the acetyl group into GlcNAc-P and UDP-GlcNAc in NAGK knockout cells. Statistical significance was calculated by unpaired t-test comparing the mean incorporation of the 2 CRISPR clones and empty vector control (EV). Mean +/- SEM of three biological replicates is represented. **B)** Percent of combined UDP-GlcNAc isotopologues containing an M+6 labeled glucosamine ring or an M+5 labeled ribose from UTP, calculated from (S3E). The percent of UDP-GlcNAc containing an M+6 isotopologue is increased in NAGK knockout cells, indicating increased de novo synthesis. Notably, the percent of UDP-GlcNAc containing an M+5 isotopologue remains constant between control and knockout cells, indicating the pool of newly synthesized nucleotides is not changing. Statistical significance was calculated by unpaired t-test comparing the mean incorporation of the 3 CRISPR clones and EV. Mean +/- SEM of three biological replicates is represented. **C)** Percent of F-6-P and GlcNAc-P isotopologues containing an M+6 isotopologue from ^{13}C glucose in NAGK knockout cells. Incorporation of labeled glucose into F-6-P is unchanged in NAGK knockout cells, though the percent of GlcNAc-P containing an M+6 isotopologue is increased in NAGK knockout cells. Statistical significance was calculated by unpaired t-test comparing the mean incorporation of the 3 CRISPR clones and EV. Mean +/- SEM of three biological replicates is represented. **D)** Measurement of HBP metabolites in PANC-1 NAGK knockout cells cultured in the indicated concentrations of glutamine. Statistical significance was calculated by unpaired t-test comparing the mean incorporation of the 3 CRISPR clones and EV. Mean +/- SEM of four biological replicates is represented. For all panels, *, $p \leq 0.05$; **, $p \leq 0.01$; ***, $p \leq 0.001$.

the HBP and not into other glucose-utilizing pathways. Thus, PDA cells exhibit flexibility in UDP-GlcNAc production, via *de novo* synthesis or salvage.

This manuscript has been co-submitted with Kim et al. (2020), "Pancreatic Cancers Scavenge Hyaluronic Acid to Support Growth."

We next assessed changes in the levels of hexosamine intermediates in high and low glutamine conditions in control and clonal NAGK KO cell lines. F-6-P abundance was not different from control cells, as expected (Fig. 3D). Consistent with increased de novo synthesis in the absence of NAGK, GlcN-6-P abundance was markedly higher in NAGK knockout cells when glutamine is abundant (Fig. 3D). GlcN-6-P levels decreased in both control and NAGK KO cells upon glutamine restriction (Fig. 3D). GlcNAc-P was modestly reduced in NAGK KO cells in both high and low glutamine conditions (Fig. 3D). UDP-GlcNAc pools were not impacted by NAGK deficiency in glutamine replete conditions but were modestly reduced compared to control after glutamine limitation (Fig. 3D). Altogether, the data indicate that GlcNAc is salvaged in PDA cells in manner responsive to glutamine availability.

NAGK knockout limits tumor growth *in vivo*

To test the role of NAGK in cell proliferation, we first monitored growth of NAGK KO cells compared to controls in 2D and 3D culture, finding minimal differences (Fig. 4A, B). However, we hypothesized that NAGK loss might have a stronger effect on proliferation *in vivo* where tumor growth can be constrained by nutrient availability. To gain initial insight into whether NAGK is likely to play a functional role in PDA progression *in vivo*, we queried publicly available datasets. From analysis of publicly available microarray data (Pei et al., 2009) and gene expression data from the Cancer Genome Atlas (TCGA), we indeed found *NAGK* expression to be increased in tumor tissue relative to adjacent normal regions of the pancreas (Fig. 4C, Fig. S4A). *GFPT1* expression was also increased in tumor tissue (Fig. 4C, Fig. S4A), consistent with its regulation by mutant KRAS (Ying et al., 2012). Two other HBP genes, *PGM3* and *UAP1*, did not show significantly increased expression in PDA tumors in these datasets (Fig. 4C, Fig. S4A). We then studied the role of NAGK in tumor growth *in vivo* by injecting NAGK CRISPR KO cells into the flank of NCr nude mice (Fig. 4D). Final tumor volume and weight were markedly reduced in the absence of NAGK (Fig. 4E, F). Of note, initial tumor growth was comparable between control and

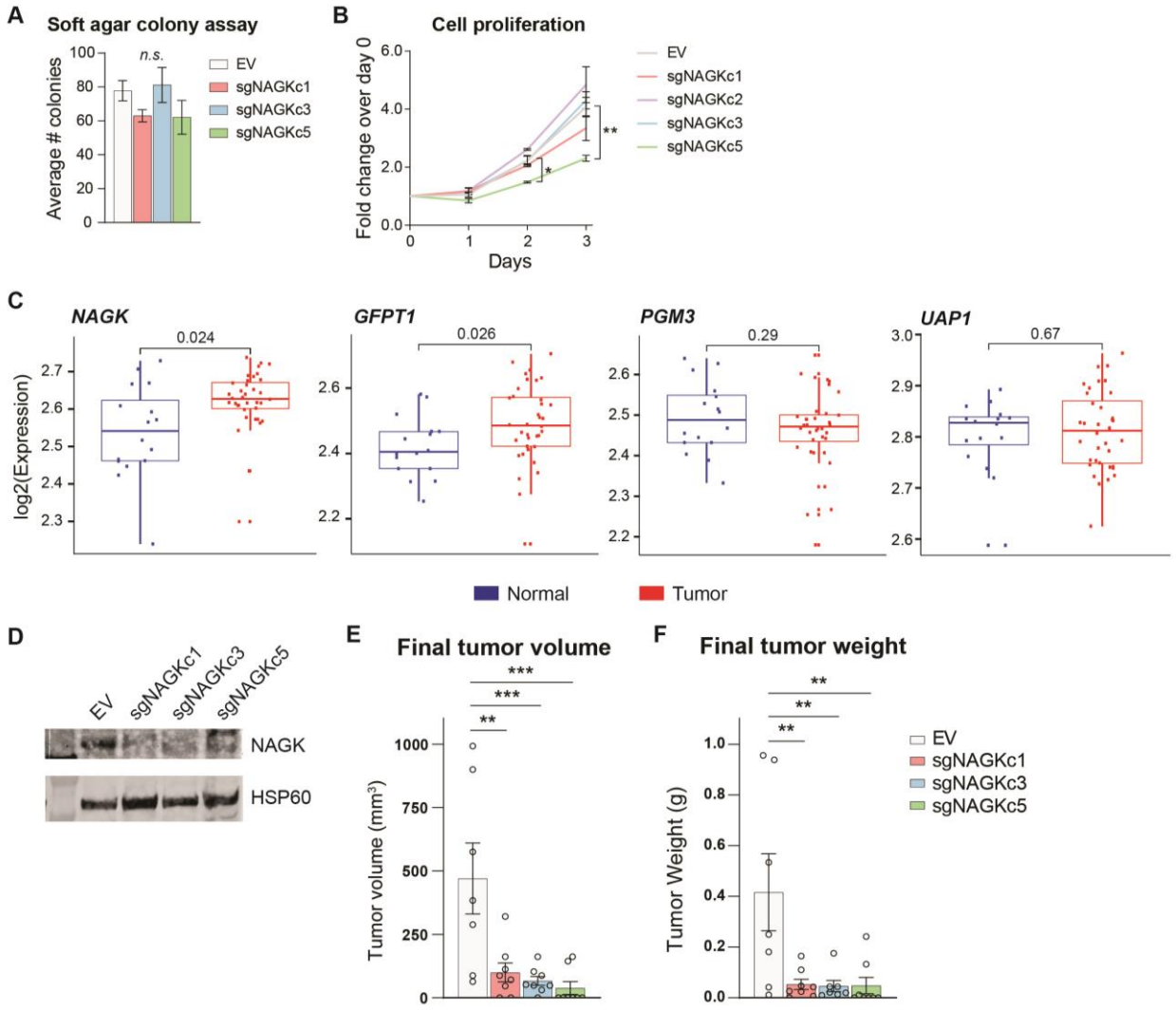

Figure 4: NAGK expression is increased in human PDA tumors and NAGK knockout reduces tumor growth *in vivo*.

A) Soft agar colony formation in NAGK knockout and control cells. Mean +/- SEM of three biological replicates is represented. **B)** 2D proliferation assay by cell count. Mean +/- SEM of three technical replicates is represented. Statistical significance was calculated using one-way ANOVA. **C)** Gene expression data for *NAGK*, *GFPT1*, *PGM3*, and *UAP1* in human PDA tumors compared with matched normal tissue. *NAGK* and *GFPT1* expression is increased in tumors, while *PGM3* and *UAP1* are consistent between tumor and normal samples. The statistical analysis was conducted by one-way ANOVA, and level of significance was defined as $p \leq 0.01$. **D)** Western blot for NAGK and HSP60 from lysate from tumors generated with the indicated cell lines, from experiment endpoint. **E)** Final tumor volume and **F)** final tumor weight of tumors generated from PANC-1 NAGK knockout cells in vivo. Cells were injected into the right flank of NCr nude mice and tumor volume was calculated from caliper measurements. Statistical significance was calculated using one-way ANOVA comparing each mean to the EV mean. Mean +/- SEM of biological replicates is represented (n = 8 each group). For all panels, *, $p \leq 0.05$; **, $p \leq 0.01$; ***, $p \leq 0.001$.

KO cells, but the NAGK knockout tumors either stopped growing or shrank while control tumors continued to grow larger (Fig. S4B), consistent with the notion that NAGK becomes more

This manuscript has been co-submitted with Kim et al. (2020), "Pancreatic Cancers Scavenge Hyaluronic Acid to Support Growth."

important as the tumors outgrow their original nutrient supply and become more dependent on scavenging and recycling. Combined, these data indicate that NAGK-mediated hexosamine salvage supports tumor growth *in vivo*.

DISCUSSION

In this study, we identify a key role for NAGK in salvaging GlcNAc for UDP-GlcNAc synthesis in PDA cells. We show that glutamine deprivation suppresses *de novo* hexosamine biosynthesis and triggers *NAGK* upregulation. *NAGK* expression is elevated in human PDA tumors, and NAGK deficiency suppresses tumor growth in mice. The data report a significant contribution of GlcNAc salvage to UDP-GlcNAc pools in PDA cells and a role for NAGK in supporting tumor growth.

This work raises several key questions for future investigation. First, the sources of GlcNAc salvaged by NAGK remain to be fully elucidated. GlcNAc may be derived from recycling of GlcNAc following O-GlcNAc removal or breakdown of a cell's own N-glycans. Additionally, GlcNAc may be recovered from the environment. Nutrient scavenging via macropinocytosis is a key feature of PDA (Commisso et al., 2013; Kamphorst et al., 2015). Macropinocytosis has mostly been associated with scavenging of protein to recover amino acids, but lysosomal break down of glycoproteins may also release sugars including GlcNAc. Further, ECM components, including hyaluronic acid (HA), which is a polymer of GlcNAc and glucuronic acid disaccharide units, may be additional sources of GlcNAc for salvage in the tumor microenvironment. Indeed, in a manuscript co-submitted with this one, Kim and colleagues identify HA as a major source of scavenged GlcNAc (Kim et al, submitted).

Further, the key fates of UDP-GlcNAc that support tumor growth remain to be elucidated. Sufficient UDP-GlcNAc is required for protein glycosylation to maintain homeostasis and prevent ER stress, particularly in a rapidly dividing cell. Additionally, a wide range of cancers exhibit

elevated O-GlcNAc, which could contribute to driving pro-tumorigenic transcriptional and signaling programs. UDP-GlcNAc is also required for HA synthesis, which is present in low amounts in normal pancreas but increases in PanIN lesions and PDA (Provenzano et al., 2012) . PDA cells are capable of producing HA in vitro (Mahlbacher et al., 1992). Depletion of fibroblasts in an autochthonous PDA mouse model results in a decrease in collagen I but not HA in the tumor microenvironment, indicating that HA must be generated by another cell type, possibly the tumor cells themselves (Özdemir et al., 2014). Previous studies demonstrated that treatment of PDA with exogenous hyaluronidase can increase vascularization and improve drug delivery to the tumor (Jacobetz et al., 2013; Provenzano et al., 2012), although a phase III clinical trial reported no improvement in overall patient survival when combining pegylated hyaluronidase with nab-paclitaxel plus gemcitabine (Cutsem et al., 2020). Recently, it was shown that inhibiting the HBP by treatment with 6-diazo-5-oxo-l-norleucine (DON) depletes HA and collagen in an orthotopic mouse model. DON treatment also increased CD8 T-cell infiltration into the tumor, sensitizing the tumor to anti-PD1 therapy (Sharma et al., 2020). Thus, targeting the HBP holds promise for improving the efficacy of other therapeutics. The findings of the current study suggest that in addition to de novo hexosamine synthesis, targeting of hexosamine salvage warrants further investigation in terms of potential for therapeutic intervention. Of note, an inhibitor targeting PGM3, which converts GlcNAc-6-P to GlcNAc-1-P and is thus required for both de novo UDP-GlcNAc synthesis and GlcNAc recycling, showed efficacy in treating gemcitabine-resistant patient-derived xenograft PDA models (Ricciardiello et al., 2020), as well as in breast cancer xenografts (Ricciardiello et al., 2018).

Finally, almost nothing is currently known about the role of NAGK and GlcNAc salvage in normal physiology. Even in non-cancerous IL-3-dependent hematopoietic cells, a substantial proportion of the UDP-GlcNAc pool remains unlabeled from ^{13}C-glucose (Wellen et al., 2010), suggesting that salvage may contribute to UDP-GlcNAc pools in a variety of cell types. However, while

GFPT1 is required for embryonic development in mice, NAGK knockout mouse embryos are viable (Dickinson et al., 2016). NAGK deficiency has not yet been characterized in postnatal or adult mice. Perhaps GlcNAc salvage is dispensable when nutrients are available and cells are not dividing, as in most healthy tissues. However, in a tumor, in which cells are proliferating and nutrients are spread thin, NAGK and GlcNAc salvage may become more important in feeding UDP-GlcNAc pools. Related questions include through what mechanisms does glutamine deprivation lead to upregulation of NAGK and is NAGK the only enzyme capable of GlcNAc salvage? The N-[1,2-$^{13}C_2$]acetyl-D-glucosamine tracing experiments show that NAGK knockout reduces but does not abolish labeling of UDP-GlcNAc, suggesting the possibility of a second undescribed salvage mechanism. Intriguingly, we noted that ^{13}C-glucose-dependent M+6 labeling of GlcNAc-P was nearly undetectable under glutamine restriction, while M+6 labeling of UDP-GlcNAc was reduced but still substantial, hinting at the existence another pathway through which glucose can enter the UDP-GlcNAc pool. The possibility of one or more additional salvage mechanisms warrants further investigation.

In sum, we report a key role for NAGK in feeding UDP-GlcNAc pools in PDA cells and in supporting xenograft tumor growth. Further investigation will be needed to elucidate the physiological functions of NAGK, as well as the mechanisms through which it supports tumor growth and its potential role in modulating therapeutic responses.

Acknowledgements: This work was supported by R01CA174761 and R01CA228339 to K.E.W. This work was also funded in part under a grant with the Pennsylvania Department of Health to K.E.W. and I.A.B. The Department specifically disclaims responsibility for any analyses, interpretations, or conclusions. I.A.B. acknowledges support of NIH Grants P30ES013508 and P30CA016520. S.L.C. received support from T32CA115299 and F31CA217070, as well as from a Patel Family Scholar Award. H.A. was supported by post-doctoral fellowship K00CA212455. T.T. is supported by the National Cancer Institute through pre-doctoral fellowship F31CA243294

This manuscript has been co-submitted with Kim et al. (2020), "Pancreatic Cancers Scavenge Hyaluronic Acid to Support Growth."

and acknowledges the Blavatnik Family for a predoctoral fellowship. L.I. is supported by T32 GM-07229. S.T. is supported by the American Diabetes Association through post-doctoral fellowship 1-18-PDF-144.

Conflict of interest: I.A.B. is a founder of Proteoform Bio and a paid consultant for Calico, Chimerix, PTC Therapeutics, Takeda Pharmaceuticals, and Vivo Capital.

This manuscript has been co-submitted with Kim et al. (2020), "Pancreatic Cancers Scavenge Hyaluronic Acid to Support Growth."

REFERENCES

Akella, N. M., Ciraku, L., & Reginato, M. J. (2019). Fueling the fire: Emerging role of the hexosamine biosynthetic pathway in cancer. *BMC Biology*, *17*(1), 1–14. https://doi.org/10.1186/s12915-019-0671-3

American Cancer Society. *Cancer Facts & Figures 2019.* Atlanta: American Cancer Society; 2019.

Caldwell, S. a, Jackson, S. R., Shahriari, K. S., Lynch, T. P., Sethi, G., Walker, S., … Reginato, M. J. (2010). Nutrient sensor O-GlcNAc transferase regulates breast cancer tumorigenesis through targeting of the oncogenic transcription factor FoxM1. *Oncogene*, *29*(19), 2831–2842. https://doi.org/10.1038/onc.2010.41

Chen, R., Lai, L. A., Sullivan, Y., Wong, M., Wang, L., Riddell, J., … Pan, S. (2017). Disrupting glutamine metabolic pathways to sensitize gemcitabine-resistant pancreatic cancer. *Scientific Reports*, *7*(1), 1–14. https://doi.org/10.1038/s41598-017-08436-6

Commisso, C., Davidson, S. M., Soydaner-Azeloglu, R. G., Parker, S. J., Kamphorst, J. J., Hackett, S., … Bar-Sagi, D. (2013). Macropinocytosis of protein is an amino acid supply route in Ras-transformed cells. *Nature*, *497*(7451), 633–637. https://doi.org/10.1038/nature12138

Cutsem, E. Van, Tempero, M. A., Sigal, D., Oh, D., Fazio, N., Macarulla, T., … Bullock, A. (2020). Randomized Phase III Trial of Pegvorhyaluronidase Alfa With Nab-Paclitaxel Plus Gemcitabine for Patients With Hyaluronan-High Metastatic Pancreatic Adenocarcinoma abstract. *Journal of Clinical Oncology*. https://doi.org/10.1200/JCO.20.00590

Dennis, J. W., & Laferte, S. (1989). Oncodevelopmental expression of -GlcNAcβ1-6Manα1-6Manβ1-branched asparaginelinked oligosaccharides in murine tissues and human breast

This manuscript has been co-submitted with Kim et al. (2020), "Pancreatic Cancers Scavenge Hyaluronic Acid to Support Growth."

carcinomas. *Cancer Research, Vol. 49*, (16), 945–950.

Dennis, J W, Laferte, S., & Vanderelst, I. (1989). Asparagine-linked oligosaccharides in malignant tumour growth. *Biochem Soc Trans*, *17*(1), 29–31. Retrieved from http://www.ncbi.nlm.nih.gov/pubmed/2714513

Dennis, James W, Laferté, S., Waghorne, C., Breitman, M. L., Kerbel, R. S., Dennis, J. W., … Kerbel, R. S. (1987). Beta1-6 Branching of Asn-Linked Oligosaccharides is Directly Associated with Metastasis, *236*(4801), 582–585.

Denzel, M. S., & Antebi, A. (2015). Hexosamine pathway and (ER) protein quality control. *Current Opinion in Cell Biology*, *33*(Figure 1), 14–18. https://doi.org/10.1016/j.ceb.2014.10.001

Dickinson, M. E., Flenniken, A. M., Ji, X., Teboul, L., Wong, M. D., White, J. K., … Murakami, A. (2016). High-throughput discovery of novel developmental phenotypes. *Nature*, *537*(7621), 508–514. https://doi.org/10.1038/nature19356

Doench, J. G., Fusi, N., Sullender, M., Hegde, M., Vaimberg, E. W., Donovan, K. F., … Root, D. E. (2016). Optimized sgRNA design to maximize activity and minimize off-target effects of CRISPR-Cas9. *Nature Biotechnology*, *34*(2), 184–191. https://doi.org/10.1038/nbt.3437

Edgar, R., Domrachev, M., & Lash, A. E. (2002). Gene Expression Omnibus: NCBI gene expression and hybridization array data repository. *Nucleic Acids Research*, *30*(1), 207–210. https://doi.org/10.1093/nar/30.1.207

Fernandes, B., Sagman, U., Auger, I. V. I., Demetrio, M., & Dennis, J. W. (1991). beta1-6Branched Oligosaccharides Breast and Colon Neoplasia1 as a Marker of Tumor Progression in Human. *Cancer Research*, *51*, 718–723.

Ferrer, C. M., Lu, T. Y., Bacigalupa, Z. A., Katsetos, C. D., Sinclair, D. A., & Reginato, M. J.

(2017). O-GlcNAcylation regulates breast cancer metastasis via SIRT1 modulation of FOXM1 pathway. *Oncogene*, *36*(4), 559–569. https://doi.org/10.1038/onc.2016.228

Granovsky, M., Fata, J., Pawling, J., Muller, W. J., Khokha, R., & Dennis, J. W. (2000). Suppression of tumor growth and metastasis in Mgat5-deficient mice. *Nature Medicine*, *6*(3), 306–312. https://doi.org/10.1038/73163

Gu, Y., Mi, W., Ge, Y., Liu, H., Fan, Q., Han, C., … Yu, W. (2010). GlcNAcylation plays an essential role in breast cancer metastasis. *Cancer Research*, *70*(15), 6344–6351. https://doi.org/10.1158/0008-5472.CAN-09-1887

Guillaumond, F., Leca, J., Olivares, O., Lavaut, M.-N., Vidal, N., Berthezène, P., … Vasseur, S. (2013). Strengthened glycolysis under hypoxia supports tumor symbiosis and hexosamine biosynthesis in pancreatic adenocarcinoma. *Proceedings of the National Academy of Sciences of the United States of America*, *110*(10), 3919–3924. https://doi.org/10.1073/pnas.1219555110

Guo, H., Zhang, B., Nairn, A. V., Nagy, T., Moremen, K. W., Buckhaults, P., & Pierce, M. (2017). O-Linked N-Acetylglucosamine (O-GlcNAc) Expression Levels Epigenetically Regulate Colon Cancer Tumorigenesis by Affecting the Cancer Stem Cell Compartment via Modulating Expression of Transcriptional Factor MYBL1. *Journal of Biological Chemistry*, *292*(10), 4123–4137. https://doi.org/10.1074/jbc.M116.763201

Guo, L., Worth, A. J., Mesaros, C., Snyder, N. W., Jerry, D., & Blair, I. A. (2016). Diisopropylethylamine/hexafluoroisopropanol-mediated ion- pairing UHPLC-MS for phosphate and carboxylate metabolite analysis: utility for studying cellular metabolism. *Rapid Commun Mass Spectrom.*, *30*(16), 1835–1845. https://doi.org/10.1002/rcm.7667.Diisopropylethylamine/hexafluoroisopropanol-mediated

This manuscript has been co-submitted with Kim et al. (2020), "Pancreatic Cancers Scavenge Hyaluronic Acid to Support Growth."

Halbrook, C. J., & Lyssiotis, C. A. (2017). Employing Metabolism to Improve the Diagnosis and Treatment of Pancreatic Cancer. *Cancer Cell*, *31*(1), 5–19. https://doi.org/10.1016/j.ccell.2016.12.006

Housley, M. P., Rodgers, J. T., Udeshi, N. D., Kelly, T. J., Shabanowitz, J., Hunt, D. F., … Hart, G. W. (2008). O-GlcNAc regulates FoxO activation in response to glucose. *Journal of Biological Chemistry*, *283*(24), 16283–16292. https://doi.org/10.1074/jbc.M802240200

Howlader, N., Noone, A.M., Krapcho, M., Miller, D., Brest, A., Yu, M., …Cronin, K.A. (eds). SEER Cancer Statistics Review, 1975-2017, National Cancer Institute. Bethesda, MD, https://seer.cancer.gov/csr/1975_2017/, based on November 2019 SEER data submission, posted to the SEER website, April 2020.

Jacobetz, M. A., Chan, D. S., Neesse, A., Bapiro, T. E., Cook, N., Frese, K. K., … Tuveson, D. A. (2013). Hyaluronan impairs vascular function and drug delivery in a mouse model of pancreatic cancer. *Gut*, *62*(1), 112–120. https://doi.org/10.1136/gutjnl-2012-302529

Kamphorst, J. J., Nofal, M., Commisso, C., Hackett, S. R., Lu, W., Grabocka, E., … Rabinowitz, J. D. (2015). Human Pancreatic Cancer Tumors Are Nutrient Poor and Tumor Cells Actively Scavenge Extracellular Protein. *Cancer Research*, *75*(3), 544–553. https://doi.org/10.1158/0008-5472.CAN-14-2211

Lau, K. S., Partridge, E. A., Grigorian, A., Silvescu, C. I., Reinhold, V. N., Demetriou, M., & Dennis, J. W. (2007). Complex N-Glycan Number and Degree of Branching Cooperate to Regulate Cell Proliferation and Differentiation. *Cell*, *129*(1), 123–134. https://doi.org/10.1016/j.cell.2007.01.049

Li, J., Byrne, K.T., Yan, F., Yamazoe, T., Chen, Z., Baslan, T., …Vonderheide, R.H., Stanger, B.Z. (2018). Tumor Cell-Intrinsic Factors Underlie Heterogeneity of Immune Cell Infiltration

This manuscript has been co-submitted with Kim et al. (2020), "Pancreatic Cancers Scavenge Hyaluronic Acid to Support Growth."

and Response to Immunotherapy. *Immunity*, 49(1), 178-193. https://doi.org/10.1016/j.immuni.2018.06.006

Li, D., Li, Y., Wu, X., Li, Q., Yu, J., Gen, J., & Zhang, X.-L. (2008). Knockdown of Mgat5 Inhibits Breast Cancer Cell Growth with Activation of CD4 + T Cells and Macrophages . *The Journal of Immunology*, *180*(5), 3158–3165. https://doi.org/10.4049/jimmunol.180.5.3158

Lynch, T. P., Ferrer, C. M., Jackson, S. R. E., Shahriari, K. S., Vosseller, K., & Reginato, M. J. (2012). Critical role of O-linked β-N-acetylglucosamine transferase in prostate cancer invasion, angiogenesis, and metastasis. *Journal of Biological Chemistry*, *287*(14), 11070–11081. https://doi.org/10.1074/jbc.M111.302547

Lyssiotis, C. A., & Kimmelman, A. C. (2017). Metabolic Interactions in the Tumor Microenvironment. *Trends in Cell Biology*, *27*(11), 863–875. https://doi.org/10.1016/j.tcb.2017.06.003

Mahlbacher, V., Sewing, A., Elsässer, H. P., & Kern, H. F. (1992). Hyaluronan is a secretory product of human pancreatic adenocarcinoma cells. *European Journal of Cell Biology*, *58*(1), 28—34. Retrieved from http://europepmc.org/abstract/MED/1644063

Mereiter, S., Balmaña, M., Campos, D., Gomes, J., & Reis, C. A. (2019). Glycosylation in the Era of Cancer-Targeted Therapy: Where Are We Heading? *Cancer Cell*, *36*(1), 6–16. https://doi.org/10.1016/j.ccell.2019.06.006

Moloughney, J. G., Kim, P. K., Vega-cotto, N. M., Rabinowitz, J. D., Werlen, G., Moloughney, J. G., … Adlam, M. (2016). mTORC2 Responds to Glutamine Catabolite Levels to Modulate the Hexosamine Biosynthesis Enzyme GFAT1. *Molecular Cell*, 1–16. https://doi.org/10.1016/j.molcel.2016.07.015

Moseley, H. N. B., Lane, A. N., Belshoff, A. C., Higashi, R. M., & Fan, T. W. M. (2011). A novel

deconvolution method for modeling UDP-N-acetyl-D-glucosamine biosynthetic pathways based on 13C mass isotopologue profiles under non-steady-state conditions. *BMC Biology*, *9*(May). https://doi.org/10.1186/1741-7007-9-37

Özdemir, B. C., Pentcheva-Hoang, T., Carstens, J. L., Zheng, X., Wu, C. C., Simpson, T. R., … Kalluri, R. (2014). Depletion of carcinoma-associated fibroblasts and fibrosis induces immunosuppression and accelerates pancreas cancer with reduced survival. *Cancer Cell*, *25*(6), 719–734. https://doi.org/10.1016/j.ccr.2014.04.005

Park, S. Y., Kim, H. S., Kim, N. H., Ji, S., Cha, S. Y., Kang, J. G., … Cho, J. W. (2010). Snail1 is stabilized by O-GlcNAc modification in hyperglycaemic condition. *EMBO Journal*, *29*(22), 3787–3796. https://doi.org/10.1038/emboj.2010.254

Pei, H., Li, L., Fridley, B. L., Jenkins, G. D., Kalari, K. R., Lingle, W., … Wang, L. (2009). FKBP51 Affects Cancer Cell Response to Chemotherapy by Negatively Regulating Akt. *Cancer Cell*, *16*(3), 259–266. https://doi.org/10.1016/j.ccr.2009.07.016

Provenzano, P. P., Cuevas, C., Chang, A. E., Goel, V. K., Von Hoff, D. D., & Hingorani, S. R. (2012). Enzymatic Targeting of the Stroma Ablates Physical Barriers to Treatment of Pancreatic Ductal Adenocarcinoma. *Cancer Cell*, *21*(3), 418–429. https://doi.org/10.1016/j.ccr.2012.01.007

Rahib, L., Smith, B. D., Aizenberg, R., Rosenzweig, A. B., Fleshman, J. M., & Matrisian, L. M. (2014). Projecting cancer incidence and deaths to 2030: The unexpected burden of thyroid, liver, and pancreas cancers in the united states. *Cancer Research*, *74*(11), 2913–2921. https://doi.org/10.1158/0008-5472.CAN-14-0155

Ricciardiello, F., Gang, Y., Palorini, R., Li, Q., Giampà, M., Zhao, F., … Chiaradonna, F. (2020). Hexosamine pathway inhibition overcomes pancreatic cancer resistance to gemcitabine

through unfolded protein response and EGFR-Akt pathway modulation. *Oncogene*, 4103–4117. https://doi.org/10.1038/s41388-020-1260-1

Ricciardiello, F., Votta, G., Palorini, R., Raccagni, I., Brunelli, L., Paiotta, A., … Chiaradonna, F. (2018). Inhibition of the Hexosamine Biosynthetic Pathway by targeting PGM3 causes breast cancer growth arrest and apoptosis. *Cell Death and Disease*, *9*(3). https://doi.org/10.1038/s41419-018-0405-4

Sanjana, N. E., Shalem, O., & Zhang, F. (2014). Sanjana, Shalem et Zhang. *Nature Medicine*, *11*(8), 783–784. https://doi.org/10.1038/nmeth.3047.Improved

Schneider, C. A., Rasband, W. S., & Eliceiri, K. W. (2012). NIH Image to ImageJ: 25 years of image analysis. *Nature Methods*, *9*(7), 671–675. https://doi.org/10.1038/nmeth.2089

Sharma, N. S., Saluja, A., Banerjee, S., Sharma, N. S., Gupta, V. K., Garrido, V. T., … Banerjee, S. (2020). Targeting tumor-intrinsic hexosamine biosynthesis sensitizes pancreatic cancer to anti-PD1 therapy Graphical abstract Find the latest version : Targeting tumor-intrinsic hexosamine biosynthesis sensitizes pancreatic cancer to anti-PD1 therapy, *130*(1), 451–465.

Steenackers, A., Olivier-Van Stichelen, S., Baldini, S. F., Dehennaut, V., Toillon, R. A., Le Bourhis, X., … Lefebvre, T. (2016). Silencing the nucleocytoplasmic O-GlcNAc transferase reduces proliferation, adhesion, and migration of cancer and fetal human colon cell lines. *Frontiers in Endocrinology*, *7*(MAY), 1–11. https://doi.org/10.3389/fendo.2016.00046

Swamy, M., Pathak, S., Grzes, K. M., Damerow, S., Sinclair, L. V, van Aalten, D. M. F., & Cantrell, D. A. (2016). Glucose and glutamine fuel protein O-GlcNAcylation to control T cell self-renewal and malignancy. *Nature Immunology*, *17*(April), 1–11. https://doi.org/10.1038/ni.3439

This manuscript has been co-submitted with Kim et al. (2020), "Pancreatic Cancers Scavenge Hyaluronic Acid to Support Growth."

Tang, Z., Kang, B., Li, C., Chen, T., & Zhang, Z. (2019). GEPIA2: an enhanced web server for large-scale expression profiling and interactive analysis. *Nucleic Acids Research*, *47*(W1), W556–W560. https://doi.org/10.1093/nar/gkz430

Taylor, R. P., Parker, G. J., Hazel, M. W., Soesanto, Y., Fuller, W., Yazzie, M. J., & McClain, D. A. (2008). Glucose deprivation stimulates O-GlcNAc modification of proteins through up-regulation of O-linked N-acetylglucosaminyltransferase. *Journal of Biological Chemistry*, *283*(10), 6050–6057. https://doi.org/10.1074/jbc.M707328200

Trefely, S., Ashwell, P., & Snyder, N. W. (2016). FluxFix: Automatic isotopologue normalization for metabolic tracer analysis. *BMC Bioinformatics*, *17*(1), 1–8. https://doi.org/10.1186/s12859-016-1360-7

Wellen, K. E., Lu, C., Mancuso, A., Lemons, J. M. S., Ryczko, M., Dennis, J. W., … Thompson, C. B. (2010). The hexosamine biosynthetic pathway couples growth factor-induced glutamine uptake to glucose metabolism. *Genes and Development*, *24*(24), 2784–2799. https://doi.org/10.1101/gad.1985910

Ying, H., Kimmelman, A. C., Lyssiotis, C. A., Hua, S., Chu, G. C., Fletcher-Sananikone, E., … Depinho, R. A. (2012). Oncogenic kras maintains pancreatic tumors through regulation of anabolic glucose metabolism. *Cell*, *149*(3), 656–670. https://doi.org/10.1016/j.cell.2012.01.058

Zhou, X., Chen, H., Wang, Q., Zhang, L., & Zhao, J. (2011). Knockdown of Mgat5 inhibits CD133+ human pulmonary adenocarcinoma cell growth in vitro and in vivo. *Clinical and Investigative Medicine. Médecine Clinique et Experimentale*, *34*(3), E155-62. Retrieved from http://www.ncbi.nlm.nih.gov/pubmed/21631992

This manuscript has been co-submitted with Kim et al. (2020), "Pancreatic Cancers Scavenge Hyaluronic Acid to Support Growth."

This manuscript has been co-submitted with Kim et al. (2020), "Pancreatic Cancers Scavenge Hyaluronic Acid to Support Growth."

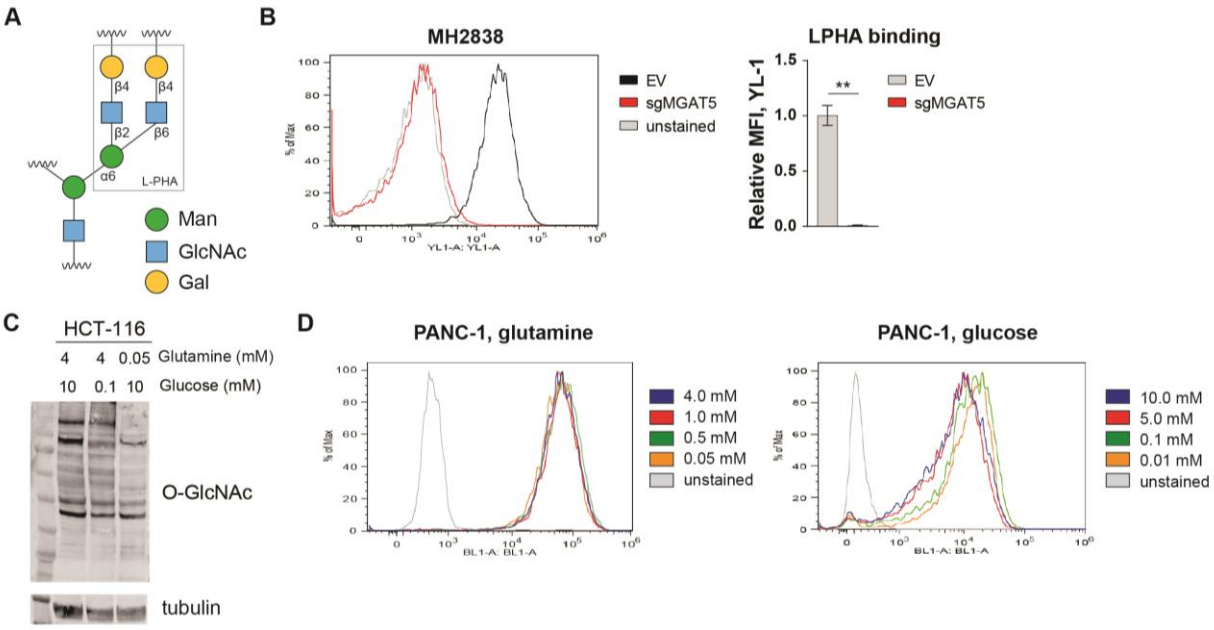

Supplemental Figure 1: LPHA binding detects MGAT5-dependent glycans.

A) Diagram of LPHA binding. LPHA recognizes specifically the β1-6 linkage established by MGAT5. **B)** LPHA binding on MGAT5 knock-out cells isolated from a KPCY tumor (Li, Byrne et al., 2018), representative flow plot and quantification. Statistical significance was calculated by unpaired t-test. **C)** O-GlcNAc levels in HCT-116 cells in high and low nutrients; cells were incubated in indicated concentrations of glucose and glutamine for 48 hours. **D)** Representative flow plots for LPHA binding graphed in Fig. 1C, D on Panc-1 cells in low glucose and low glutamine. Panels C) and D) are representative of at least two independent experimental replicates. *, $p \leq 0.05$; **, $p \leq 0.01$; **, $p \leq 0.001$.

This manuscript has been co-submitted with Kim et al. (2020), "Pancreatic Cancers Scavenge Hyaluronic Acid to Support Growth."

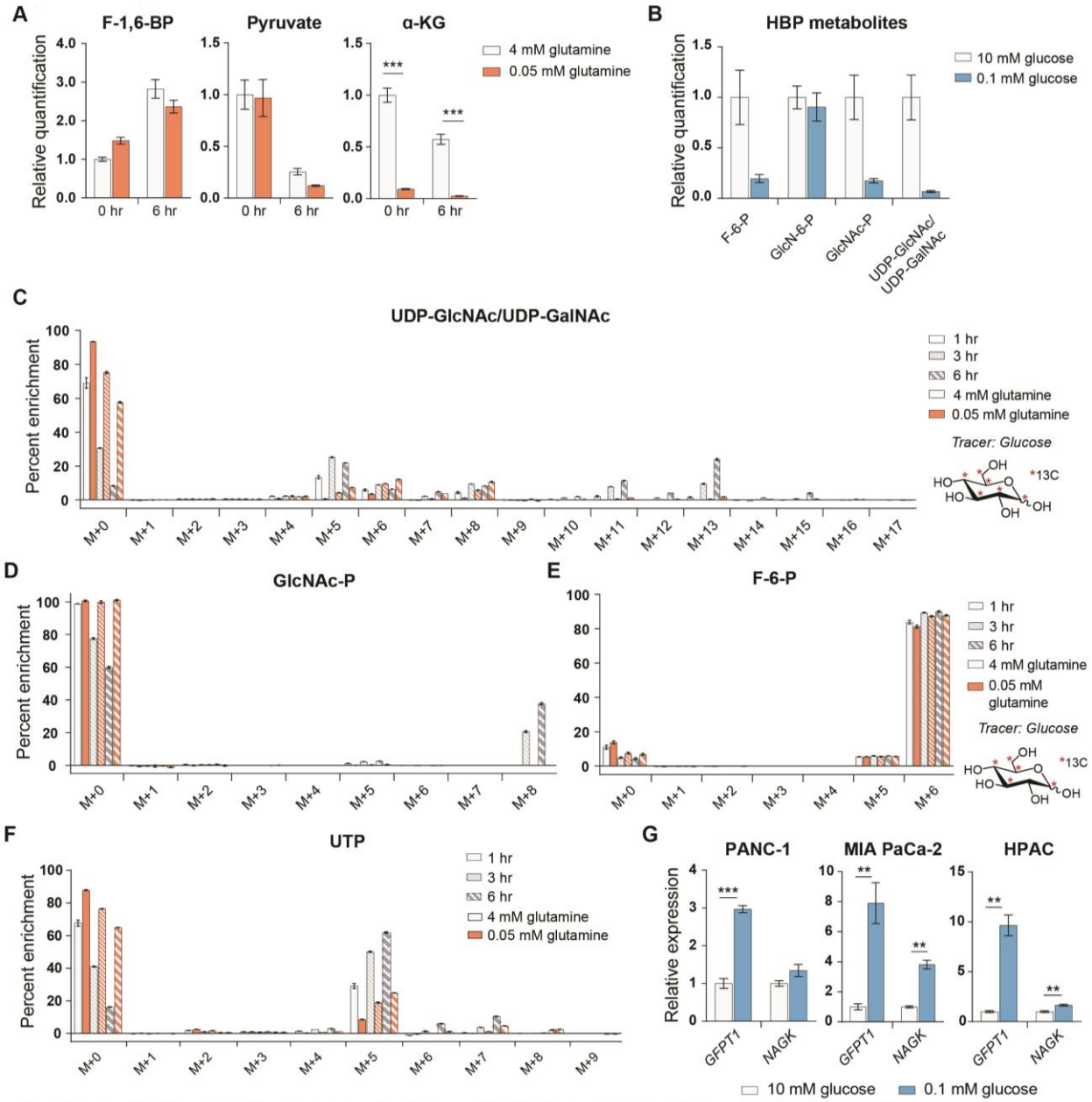

Supplemental Figure 2: *De novo* hexosamine synthesis is suppressed in low glutamine conditions.

A) Measurement of fructose-1,6-bisphosphate (F-1,6-BP), pyruvate, and alpha-ketoglutarate (α-KG) in PANC-1 cells after culture for 48 hours in 0.05 mM glutamine. Statistical significance was calculated by unpaired t-test. Mean +/- SEM of five biological replicates is represented. B) Measurement of HBP metabolites in PANC-1 cells after culture for 48 hours in 0.1 mM glucose. Mean +/- SEM of five biological replicates is represented. C) Measurement of ^{13}C glucose incorporation into UDP-GlcNAc in high and low glutamine. Mean +/- SEM of three biological replicates is represented. D) Measurement of ^{13}C glucose incorporation into GlcNAc-P in high and low glutamine. Mean +/- SEM of three biological replicates is represented. E) Measurement of ^{13}C glucose incorporation into fructose-6-phosphate in high and low glutamine Mean +/- SEM of three biological replicates is represented. F) Measurement of ^{13}C glucose incorporation into UTP in high and low glutamine. Mean +/- SEM of three biological replicates is represented. G) Gene expression of *GFPT1* and *NAGK* in PDA cells cultured in the indicated concentrations of glucose for 24 hours. Statistical significance was calculated by unpaired t-test. Mean +/- SEM of three biological replicates is represented. All panels are representative of at least 2 independent experimental replicates. *, $p \leq 0.05$; **, $p \leq 0.01$; ***, $p \leq 0.001$.

This manuscript has been co-submitted with Kim et al. (2020), "Pancreatic Cancers Scavenge Hyaluronic Acid to Support Growth."

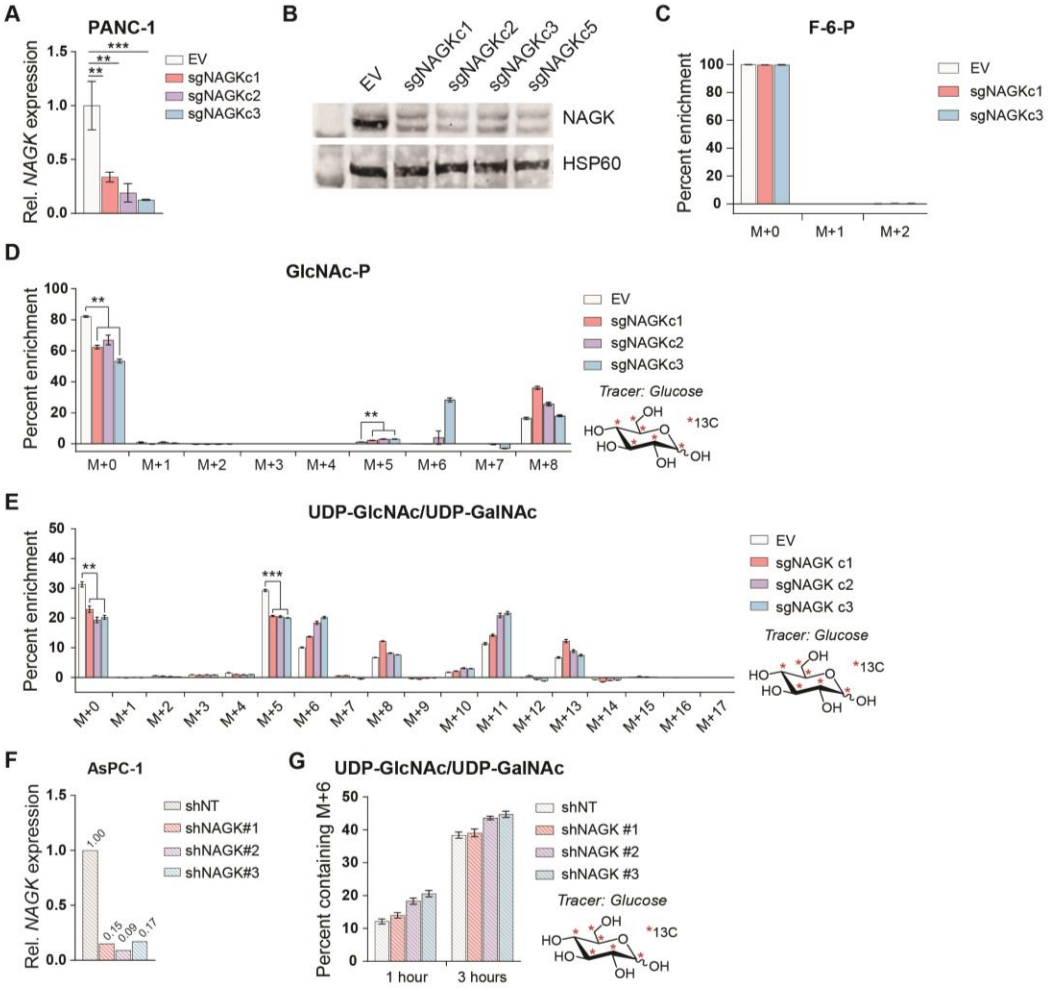

Supplemental Figure 3: NAGK silencing alters glucose incorporation into HBP intermediates.

A) *NAGK* gene expression in EV versus NAGK CRISPR knockout cells. Statistical significance was calculated using one-way ANOVA. Mean +/- SEM of three biological replicates is represented. **B)** Western blot for NAGK and HSP60 from lysate generated from NAGK CRISPR knockout cells. **C)** Incorporation of ^{13}C GlcNAc labeled on the acetyl group into F-6-P in NAGK knockout cells. No labeling from ^{13}C GlcNAc is expected in F-6-P. Mean +/- SEM of three biological replicates is represented. **D)** Incorporation of ^{13}C glucose into GlcNAc-P in NAGK knockout cells. Statistical significance was calculated by unpaired t-test comparing the mean incorporation of the 3 CRISPR clones and the EV. Mean +/- SEM of three biological replicates is represented. **E)** Incorporation of ^{13}C glucose into UDP-GlcNAc in NAGK knockout cells. Statistical significance was calculated by unpaired t-test comparing the mean incorporation of the 3 CRISPR clones and the EV. Mean +/- SEM of three biological replicates is represented. **F)** Expression of NAGK in AsPC-1 cells with shRNA knockdown. **G)** Percent of UDP-GlcNAc containing an m+6 labeled glucosamine ring in PANC-1 cells with shRNA targeting NAGK. The fraction is calculated from measurement of ^{13}C glucose incorporation into UDP-GlcNAc. Mean +/- SEM of three biological replicates is represented. All panels are representative of at least two independent experimental replicates. *, $p \leq 0.05$; **, $p \leq 0.01$; ***, $p \leq 0.001$.

This manuscript has been co-submitted with Kim et al. (2020), "Pancreatic Cancers Scavenge Hyaluronic Acid to Support Growth."

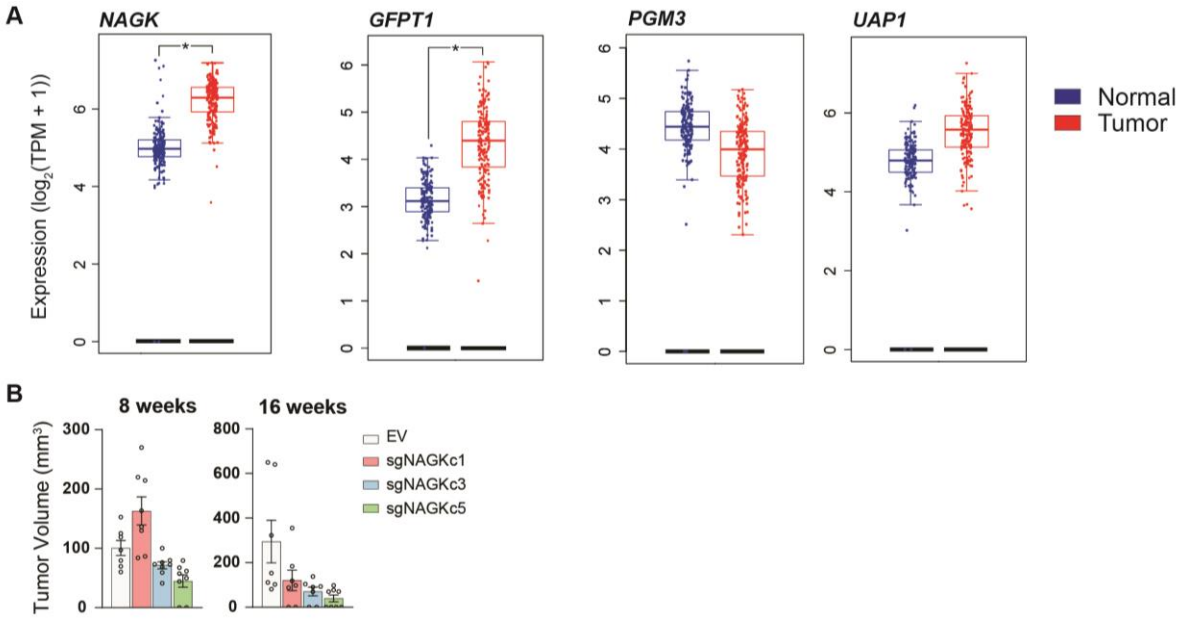

Supplemental Figure 4: NAGK knockout does not impair initial tumor growth but ultimately limits tumor growth *in vivo*.

A) Gene expression data plotted using GEPIA2 comparing TCGA pancreatic cancer samples with TCGA normal pancreas samples and GTEx data. Differential analysis between tumor and normal tissues was analyzed by one-way ANOVA. *, p<0.05. **B)** Tumor volume of NAGK knockout tumors at earlier time points in the experiment. Initial growth of NAGK knockout cells in vivo was compara ble to control cells, but over time NAGK knockout tumors either stopped growing or regressed.

This manuscript has been co-submitted with Kim et al. (2020), "Pancreatic Cancers Scavenge Hyaluronic Acid to Support Growth."